Pergamon

*Int. J. Multiphase Flow* Vol. 23, No. 6, pp. 1171–1188, 1997

Printed in Great Britain
0301-9322/97 $17.00 + 0.00

PII: S0301-9322(97)00023-2

# STUDY INTO NUCLEATION OF STEAM DURING EXPANSION THROUGH A NOZZLE

G. CINAR[1], B. S. YILBAS[2] and M. SUNAR[2]

[1]Erciyes Universitesi, Kayseri, Turkey
[2]King Fahd University of Petroleum and Minerals, Dhahran 31261, Saudi Arabia

*(Received 17 January 1996; in revised form 17 March 1997)*

**Abstract**—The development of nucleation theory makes possible to predict droplet formation in expanding steam. The present study is conducted to investigate the nucleation process occurring during the flow through convergent–divergent nozzles. A kinetic theory approach for determining the rate of droplet growth has been developed successfully. The governing flow equations are developed for the free and continuous flow regimes. A numerical scheme is introduced to solve the resulting equations. To validate the predictions, an experiment is carried out to measure the droplet size and thermodynamic properties of steam expanding through a convergent–divergent nozzle. It is found that the amount of supersaturation is limited with pressure increase and the limiting degrees of supercooling and the resulting droplet sizes depend on the Wilson pressure and the expansion rate. The theoretical predictions are in good agreement with the experimental measurements and the process of nucleation in high pressure steam can, possibly, be described satisfactorily by the model developed in the present study. © 1997 Elsevier Science Ltd.

*Key Words:* nucleation, expansion through a nozzle, droplet formation

## 1. INTRODUCTION

Wetness losses play an important role in determining the efficiency of the wet stages of steam turbines. This may be due to departures from thermodynamic equilibrium due to the existence of two-phase flow in turbine passages that affect the performance of the steam turbine. The release of latent heat associated with return to equilibrium can affect the behavior of the parent compressible vapor. The development of the nucleation theory enhanced the study of the wetness problem in steam turbines, in combination with the gas dynamic equations, which allow nucleation and wet steam flows to be treated analytically. Consequently, the analytical prediction of properties of subcooled flow through orifices, short pipes and nozzles has been tackled by incorporating nucleation models into the equations for frictionless and homogeneous flow (Bahter and Heaton 1988). Various approaches have been used for defining nucleation superheat criteria and the models developed appear to predict the two-phase flow regime after measuring the void fractions, pressure distributions and mass flow rates.

Flow through an enclosure has been investigated (Yeoh and Young 1984) using the streamline curvature method; the authors faced difficulties in treating the choking conditions at the throat. The characteristics of a flow with spontaneous condensation of steam in supersonic nozzles were studied (Filippov *et al.* 1980). They predicted the droplet size distribution within acceptable accuracy.

On the experimental side, droplet size measurement in steam turbine was carried out (Tatsuno and Nagao 1986) using an optical fiber droplet sizer. They have shown that the average droplet diameters were between 0.2 and 0.1 $\mu$m, measured at wetnesses of 6–14%, and this varied with the radial direction of the blades. Condensation of steam down-flow inside a vertical tube and the hydraulic resistance were investigated (Lokshin *et al.* 1984). They considered only high mass velocities and measured the total pressure differential due to various mass velocities. In addition, the total pressure drop with downflow of steam condensing in a vertical tube was studied (Labuntsov *et al.* 1984). They have shown that within the experimental range, the total drop in

pressure with down-flow of condensing saturated steam and the loss in pressure drop due to friction were independent of tube diameter.

In light of the above findings, the present study investigates the nucleation mechanisms taking place during flow through convergent–divergent nozzles. The flow equations are developed to compute the pressure, expansion rate and the droplet formation along the nozzle. Two regimes of flow are considered, namely free molecular and continuous flow regimes. A numerical technique is employed to solve the governing equations. An experiment is conducted to validate the theoretical predictions: it is an experimental investigation into the wetness problem due to expansion of steam through a convergent–divergent nozzle. The pressure distribution along the nozzle is measured for both dry and wet steam conditions. The experiment is extended to include different stagnation pressures and stagnation temperatures. This provides an extended view of the expansion phenomenon through the nozzle.

## 2. MATHEMATICAL MODELING OF THE GOVERNING EQUATIONS

The governing equations of the flow are developed for steam flowing in a convergent–divergent nozzle and the relevant equations are given under the following subheadings.

### 2.1. Mass continuity

The continuity equation for two phase-flow in case of steady state may be written as

$$\dot{m}_{tot} = \dot{m}_L + \rho_G A V_G = \text{constant}, \qquad [1]$$

where $\dot{m}_{tot}$ is the total mass flow rate, $\dot{m}_L$ and $\rho_G A V_G$ are the mass flow rates of the liquid and gas phases, respectively. It is assumed that the volume of the liquid phase is negligible as compared to the volume of the gas phase. The differentiation of [1] yields

$$\frac{d\rho_G}{\rho_G} + \frac{dA}{A} + \frac{dV_G}{V_G} + \frac{d\dot{m}_L}{\dot{m}_{tot} - \dot{m}_L} = 0. \qquad [2]$$

### 2.2. Momentum equation

The momentum change across an element $dx$ in the flow direction, considering the frictional and pressure forces, is

$$d[\dot{m}_G V_G + \dot{m}_L V_G] = -A\, dP - \frac{fA\rho_G V_G^2}{2d_e} dx, \qquad [3]$$

where $f$ is an appropriate friction factor and $d_e$ is the duct hydraulic diameter, which is

$$d_e = \frac{4A}{\text{wetted perimeter}}$$

and $V_G$ and $V_L$ are the velocities of the gas and liquid phases, respectively. Assuming no slip occurrence between the phases (i.e. $V_G = V_L$) and introducing the square of the Mach number ($N = M^2 = V_G^2 \rho_G / kP$, where $k$ is the specific heat ratio given in the appendix) into [3], yields

$$\frac{dP}{P} = -\frac{kN}{(1-X)} \frac{dV_G}{V_G} - \frac{kfN}{2d_e} dx, \qquad [4]$$

where $X$ is the wetness fraction defined as

$$X = \frac{T_G}{P} \left( \frac{\partial P}{\partial T_G} \right) \rho_G.$$

*2.3. Energy equation*

The energy equation for steady state adiabatic flow can be written as

$$\mathrm{d}\left[\dot{m}_G\left(h_G + \frac{V_G^2}{2}\right) + \dot{m}_L\left(h_L + \frac{V_L^2}{2}\right)\right] = 0, \quad [5]$$

where $h_G$ and $h_L$ are the gas and liquid phase enthalpies, respectively. Knowing that $\dot{m}_G = \dot{m}_{tot} - \dot{m}_L$ and assuming $V_G = V_L$, then dividing by $\dot{m}_{tot}$ gives

$$\mathrm{d}h_G + V_G \mathrm{d}V_G - h_{LG}\frac{\mathrm{d}\dot{m}_L}{\dot{m}_{tot}} - \dot{m}_L\frac{\mathrm{d}h_{LG}}{\dot{m}_{tot}} = 0, \quad [6]$$

where $h_{LG} = h_G - h_L$. From the properties of the steam, given in the appendix, $\mathrm{d}h_G$ can be written as

$$\mathrm{d}h_G = c_P \mathrm{d}T_G + \left(1 - \frac{\chi}{X}\right)\frac{\mathrm{d}P}{\rho_G}, \quad [7]$$

where $c_P$ (specific heat at constant pressure) is

$$c_P = \frac{k}{(k-\chi)}\frac{X^2}{\chi}\frac{P}{\rho_G T_G} \quad [8]$$

and

$$\chi = \frac{\rho_G}{P}\left(\frac{\partial P}{\partial \rho_G}\right)_{T_G}$$

and $k$ is isentropic constant for vapor phase given in the appendix. Using [7] and [8], Mach number and dividing by $c_{PT_G}$ gives

$$\frac{\mathrm{d}T_G}{T_G} + \frac{(k-\chi)}{k}\frac{(\chi - X)}{X^2}\frac{\mathrm{d}P}{P} + \frac{(k-\chi)}{X^2}\chi N\frac{\mathrm{d}V_G}{V_G} - \frac{h_{LG}}{c_P T_G}\frac{\mathrm{d}\dot{m}_L}{\dot{m}_{tot}} - \frac{\dot{m}_L}{\dot{m}_{tot}}\frac{\mathrm{d}h_{LG}}{c_P T_G} = 0. \quad [9]$$

*2.4. Mass transfer in the free molecular regime*

In the free molecular regime, it is assumed that the droplet surface is exposed to molecules with the properties of the surrounding vapor. The mass balance may be developed when considering the difference between the molecular impingement and evaporation rates from the surface. The mass rate of molecules striking the droplet and adhering to is (Frenkel 1946)

$$\left(\frac{\mathrm{d}m}{\mathrm{d}t}\right)_{adh} = q_{con} 4\pi r^2 \rho_G \sqrt{\frac{\mathrm{R}T_G}{2\pi}},$$

where $q_{con}$ is the condensation coefficient and $\rho_G$ and $T_G$ are the vapor density and temperature respectively, and $r$ is the droplet radius.

The number of molecules evaporating from the surface per unit time may be obtained when assuming that the droplet is removed to vapor environment at temperature $T_L$ and pressure $P_S(T_L, r)$, as there exists equilibrium between the phases. Therefore, the rate of molecules evaporating is

$$\left(\frac{\mathrm{d}m}{\mathrm{d}m}\right)_{evap} = q_{evap} 4\pi r^2 \rho_S(T_L, r)\sqrt{\frac{\mathrm{R}T_L}{2\pi}},$$

where $q_{evap}$ is the evaporation coefficient, $T_L$ the liquid temperature, and $\rho_S(T_L, r)$ the steam density

corresponding to the saturation pressure at temperature $T_L$ over a surface of curvature $r$. Consequently, the net rate of growth of the droplet can be expressed as

$$\frac{dm}{dt} = 4\pi r^2 \rho_L \frac{dr}{dt} = \left(\frac{dm}{dt}\right)_{adh} - \left(\frac{dm}{dt}\right)_{evap}.$$

Therefore, assuming the evaporation coefficient $q_{evap}$ equal to $q_{con}$, for the free molecular regime we obtain

$$\left(\frac{dr}{dt}\right)_{fm} = \frac{q}{\rho_L}\sqrt{\frac{R}{2\pi}}\left(\rho_G\sqrt{T_G} - \rho_s(T_L, r)\sqrt{T_L}\right). \quad [10]$$

It should be noted that at thermodynamic equilibrium, the coefficients $q_{con}$ and $q_{evap}$ are equal, but this is not necessarily so when net condensation or evaporation is occurring in a non-equilibrium thermodynamic process. For a linearized analysis,

$$\frac{\Delta P}{P} \ll 1, \quad \frac{\Delta T}{T_G} \ll 1$$

and

$$\frac{q_{evap}}{q_{con}} = 1 + \alpha_P \frac{\Delta P}{P} + \alpha_T \frac{\Delta T}{T_G},$$

where $\alpha_P$ and $\alpha_T$ are defined by

$$\alpha_P = \left[\frac{\partial(q_{evap}/q_{con})}{\partial(\Delta P/P)}\right]_{\Delta P = \Delta T = 0}$$

and

$$\alpha_T = \left[\frac{\partial(q_{evap}/q_{con})}{\partial(\Delta T/T)}\right]_{\Delta P = \Delta T = 0}$$

It was shown that $\alpha_P$ and $\alpha_T$ are not dependent and are constrained by the Onsager reciprocal relation (Young 1991). In this case,

$$\alpha_T = -\left(\frac{c}{2}\right)\alpha_P,$$

where $c$ is a constant. However, in the present experimental domain, the microscopic regions are considered, $q_{evap} = q_{con}$ can be justifiable.

### *2.5. Mass transfer in continuum regime*

The droplets can grow to a size comparable to the mean free path even at low pressure, in this case, free molecular consideration fails to predict the droplet growth rate. Transition into the continuum regime occurs and diffusion becomes the governing process. This regime is more likely to occur at high pressure steam conditions, since high densities imply short mean free paths. In the continuum regime, the mass flux of vapor condensing on a droplet may be obtained by integrating Fick's law between the droplet surface and the bulk of the vapor. After substitution in terms of the droplet growth rate, the following is obtained

$$\left(\frac{dr}{dt}\right)_{cf} = \frac{1}{\rho_L r}(\rho_G D_G - \rho' D')$$

where $\rho_G$, $D_G$ and $\rho'$, $D'$ denote the vapor density and coefficients of self diffusion in the bulk

of the vapor and next to the droplet surface, respectively. Using the relation (given in the appendix)

$$D = c\sqrt{\frac{T}{P^n}}$$

where $n = 0.8688729$, $c = 0.011441$, $T$, $P$ and $D$ are the temperature (K), pressure (Pa) and self diffusion coefficient ($m^2/s$) respectively, the droplet growth rate in the continuum regime can be written as

$$\left(\frac{dr}{dr}\right)_{cf} = \frac{2\sqrt{R}}{1.88\rho_L Sc}\,Kn(\rho_G\sqrt{T_G} - \rho_S(T_L, r)\sqrt{T_L}), \qquad [11]$$

where Sc is the Schmidt number defined as

$$Sc = \frac{\mu}{\rho D}$$

and Kn is the Knedsen number defined as

$$Kn = \frac{\bar{l}}{2r}$$

where $\bar{l}$ is the mean free path. It should be noted that according to the kinetic theory, the diffusion coefficient and viscosity may be expressed as

$$D = \frac{1}{3}\bar{l}\bar{c}$$

and

$$\mu = \frac{1}{3}\bar{l}\rho\bar{c},$$

where $\bar{c}$ is the particle averaged velocity. Equation [11] may be combined with [10] into a single equation which is valid for all flow regimes. Assuming a relationship of the form

$$\frac{dr}{dt} = \frac{1}{1 + z\,Kn}\left(\frac{dr}{dt}\right)_{cf} \qquad [12]$$

and by selecting

$$z = \frac{2\sqrt{2\pi}}{1.88q\,Sc}$$

it may be seen that for values of $Kn \ll 1$, [12] reduces to [11]. For values of $Kn \gg 1$,

$$1 + z\,Kn \to z\,Kn$$

and [12] reduces to the free molecular equation. Thus, the droplet growth equation valid for both the free and continuum flow regimes may be written as

$$\frac{dr}{dr} = \left[\frac{Kn}{1 + 0.375q\,Sc}\right]\frac{q}{\rho_L}\sqrt{\frac{R}{2\pi}}\,[\rho_G\sqrt{T_G} - \rho_S(T_L, r)\sqrt{T_L}].$$

*2.6. Vapor phase Mach number*

When integrating the governing equations of flow, it may be useful to introduce a vapor phase Mach number. The vapor phase Mach number has already been defined earlier as:

$$N = M^2 = \frac{V_G^2\rho_G}{kP}. \qquad [13]$$

Over a small increment $dx$ in the flow direction, the variation of $k$ relative to the other terms is small and, therefore, it may be regarded as constant. Differentiation of [13] gives

$$\frac{dN}{N} = 2\frac{dV_G}{V_G} + \frac{d\rho_G}{\rho_G} - \frac{dP}{P}. \qquad [14]$$

The solution of the governing equations of flow appears to be complicated. Taking

$$\frac{dA}{A}, \frac{f}{2}\frac{dx}{d_e}, \frac{d\dot{m}_L}{\dot{m}_{tot} - \dot{m}_L}, \frac{d\dot{m}_L}{\dot{m}_{tot}} \quad \text{and} \quad \frac{dh_{LG}}{c_p T_G}$$

as independent variables, the four equations [2], [4], [9] and [14] and the equation of state developed in the appendix

$$\frac{dP}{P} - \chi\frac{d\rho_G}{\rho_G} - X\frac{dT_G}{T_G} = 0 \qquad [15]$$

are sufficient to solve for five unknowns, i.e. for

$$\frac{dP}{P}, \frac{dV_G}{V_G}, \frac{d\rho_G}{\rho_G}, \frac{dT_G}{T_G} \quad \text{and} \quad \frac{dN}{N}.$$

The resulting equations for three of these unknowns are

$$\frac{dT_G}{T_G} = \frac{1}{\left[1 - \frac{N}{(1-X)}\left(1 + X\frac{(k-\chi)}{X}\right)\right]}\left[\frac{k-\chi}{X^2}(\chi - X - kN)Nf\frac{d\chi}{2d_e}\right.$$

$$\left. + \left(1 - \frac{kN}{(1-X)\chi}\right)\left(\frac{h_{LG}}{c_p T_G}\frac{d\dot{m}_L}{\dot{m}_{tot}} + \frac{\dot{m}_L}{\dot{m}_{tot}}\frac{dh_{LG}}{c_p T_G}\right) + \frac{(k-\chi)}{X^2}\left(\chi - \frac{\chi - X}{(1-X)}\right)N\left(\frac{dA}{A} + \frac{d\dot{m}_L}{\dot{m}_{tot} - \dot{m}_L}\right)\right], \qquad [16]$$

$$\frac{d\rho_G}{\rho_G} = \frac{1}{\left[1 - \frac{N}{(1-X)}\left(1 + X\frac{(k-\chi)}{X}\right)\right]}\left[\frac{-N}{X}(k - \chi + Y)\frac{f}{2d_e}\frac{d\chi}{}\right.$$

$$\left. + \frac{N}{(1-X)}\left(1 + X\frac{(k+\chi)}{X}\right)\left(\frac{dA}{A} + \frac{d\dot{m}_L}{\dot{m}_{tot} - \dot{m}_L}\right) - \frac{X}{\chi}\frac{d(h_{LG}\dot{m}_L)}{c_p T_G \dot{m}_{tot}}\right] \qquad [17]$$

and

$$\frac{dN}{N} = \frac{1}{\left[1 - \frac{N}{(1-X)}\left(1 + X\frac{(k-\chi)}{X}\right)\right]}\left[\left[\left(\frac{k-\chi}{X}\right)(kN+1) + k + 1\right]\frac{Nf}{2}\frac{d\chi}{d_e}\right.$$

$$\left. + \left(1 + \frac{kN}{(1-X)}\right)\frac{X}{\chi}\frac{d(h_{LG}\dot{m}_L)}{c_p T_G \dot{m}_{tot}} - \left[2 + \frac{N}{(1-X)}\left((k-1) - X\left(\frac{k-\chi}{X}\right)\right)\right]\left(\frac{dA}{A} + \frac{d\dot{m}_L}{\dot{m}_{tot} - \dot{m}_L}\right)\right]. \qquad [18]$$

The liquid terms $\dot{m}_L$ and $d\dot{m}_L$ have to be calculated at each integration step using the nucleation rate and droplet growth equations given above. To evaluate the liquid formed in an axial increment $\Delta x$, two groups of droplets may be identified:

(i) droplets formed within the axial increment $\Delta x$, which are known as the first-kind droplets;
(ii) droplets formed upstream of the increment $\Delta x$ continue to grow when passing through the axial increment $\Delta x$, which are known as the second-kind droplets.

The contribution of the first-kind droplets is such that new droplets appear over the axial increment $\Delta x$ at different times $i\delta t$, where $i = 1, 2, \ldots, n$ with $\Delta t = n\delta t$ and grow in the axial increment by amounts depending on their birth place. Considering constant pressure and temperature for the vapor phase over the increment $\Delta x$ the nucleation rate $J$ can be assumed as constant. Therefore, during the time increment $\Delta t$ the number of nuclei formed along $\Delta x$ per unit volume is $J\Delta t$ with $\Delta t = n\delta t$. Hence, their contribution may be expressed as

$$\mathrm{d}\dot{m}_{\mathrm{L}}(\mathrm{A}) = Jn\delta tAu\frac{4}{3}\pi\rho_{\mathrm{L}}\left(\frac{r_0^2}{2}+\frac{r_1^2}{2}+\frac{r_2^2}{2}+\cdots+\frac{r_n^2}{2}\right),$$

where $r_0, r_1, r_2, \ldots, r_n$ are the radii of the droplets leaving the increment $\Delta x$ and those were formed successively at $i = 1, 2, \ldots, n$ during the $\Delta t = n\delta t$ time increment and $u$ is the axial velocity of the flow and $A$ is the cross sectional area. The contribution of the second-kind droplets may be expressed as

$$d\dot{m}_{\mathrm{L(B)}} = N_{\mathrm{i}}\frac{4}{3}\pi\rho_{\mathrm{L}}(r_{\mathrm{e}}^2 - r_{\mathrm{i}}^2)$$

where $N_{\mathrm{i}}$ is the number of droplets passing through the increment $\Delta t$ per second and $r_{\mathrm{i}}$ is the average incoming, droplet radius defined by

$$r_{\mathrm{i}} = \left(\frac{S_{\mathrm{A}}}{4\pi N_{\mathrm{i}}}\right)^{1/2},$$

while $r_{\mathrm{e}}$ is the corresponding droplet radius at the exit of the increment $\Delta x$ and $S_{\mathrm{A}}$ is the surface area.

Consequently, the total liquid mass flow rate $\dot{m}_{\mathrm{L}}$, across the surface area $S_{\mathrm{A}}$ and the number of droplets leaving the axial increment $\Delta t$ per second become

$$\dot{m}_{\mathrm{L}} = N_{\mathrm{i}}\frac{4}{3}\pi r_{\mathrm{i}}^3\rho_{\mathrm{Li}} + \mathrm{d}\dot{m}_{\mathrm{L(A)}} + d\dot{m}_{\mathrm{L(B)}},$$

$$S_{\mathrm{A}} = N_{\mathrm{i}}4\pi r_{\mathrm{i}}^2 + J\delta tAu4\pi\left(\frac{r_0^2}{2}+\frac{r_1^2}{2}+\frac{r_2^2}{2}+\cdots+\frac{r_n^2}{2}\right)$$

and

$$N_{\mathrm{e}} = N_{\mathrm{i}} + J\Delta tAu.$$

It should be noted that the nucleation rate based on a thermal equilibrium cluster growth can be written as (Young 1991)

$$J = q\sqrt{\frac{2\sigma}{\pi m^3}}\frac{\rho_{\mathrm{G}}^2(T_{\mathrm{G}})}{\rho_{\mathrm{L}}}\exp\left(-\frac{\Delta G_{\mathrm{G}}^*}{\mathrm{K}T_{\mathrm{G}}}\right), \qquad [19]$$

where $\sigma$ is the surface tension, $q$ is the condensation coefficient, K is the Boltzmann's constant and $\Delta G_{\mathrm{G}}$ is the critical energy barrier. However, the condensation reaction taking place on the surface of growing clusters is exothermic, therefore, embryos tend to have a characteristic mean temperature above that of a single molecule in the system. This difficulty in the transport of the latent heat back to the vapor tends to retard the nucleation rate. Kantrowitz (Kantrowitz 1951) was the first to estimate the effect of this thermal non-equilibrium process on the classical nucleation rate equation [19]. He showed that [19] should be written as (Young 1991)

$$J = \frac{1}{(1+v)}q\sqrt{\frac{2\sigma}{\pi m^3}}\frac{\rho_{\mathrm{G}}^2(T_{\mathrm{G}})}{\rho_{\mathrm{L}}}\exp\left(-\frac{\Delta G_{\mathrm{G}}^*}{\mathrm{K}T_{\mathrm{G}}}\right), \qquad [20]$$

where the factor $(1 + v)$ would reflect the effects of the temperature difference between the vapor and clusters, and $v$ is given by

$$v = \frac{q\rho}{\alpha_r}\sqrt{\frac{RT}{2\pi}}\left(\frac{h_{LG}^2}{R^2T^2} - \frac{h_{LG}}{RT}\right), \quad [21]$$

where $\alpha_r$ is the heat transfer coefficient and $h_{LG} = h_G - h_L$ for non-equilibrium process.

However, when deriving [19], the partial pressure of the clusters had been omitted. Courtney (Courtney 1962) adjusted this equation and proposed a correction. The result is that [19] is reduced by a factor equal to the supersaturation ratio. Therefore

$$J = \frac{1}{(1+v)}q\sqrt{\frac{2\sigma}{\pi m^3}}\frac{\rho_G^2(T_G)}{\rho_L}\exp\left(-\frac{\Delta G_G^*}{KT_G}\right)\frac{P_s(T_G)}{P}, \quad [22]$$

where $P_s(T_G)$ is the saturation pressure corresponding to the vapor temperature. The corrections made to [19] reduce the nucleation rate. However, this effect is small, the value of $J$ is mainly dominated by the highly variable exponential factor.

## 3. EXPERIMENTAL

Figure 1 shows the experimental set up. Steam flows from the superheater to the inlet receiver where its temperature and pressure are measured, and, then, flows through the test section. Static pressure along the nozzle is sensed by a 1.83 mm bore Stodola search tube. This tube is guided axially by several supports of which two are located one on each side of the nozzle. A small vent on the pressure transducer mount is used to purge any air in the system prior to an experiment. The inlet total temperature of the steam is measured with a copper-constantan thermocouple probe inserted through a gland housing into the inlet receiver and fitted with a radiation shield. All the measuring device outputs are fed into the computer and recorded simultaneously.

A convergent–divergent cylindrical nozzle is used. The layout of the nozzle is shown in figure 2. It was manufactured from steel bar with half angles of divergence of 2.8°.

The experiment is carried out at different steam pressures and inlet temperatures (table 1). The highest value of the selected range gives an entirely dry static pressure distribution along the nozzle length, and the other settings are low enough for the typical pressure to rise due to rapid condensation occurring within a distance of approximately 50 mm downstream of the throat.

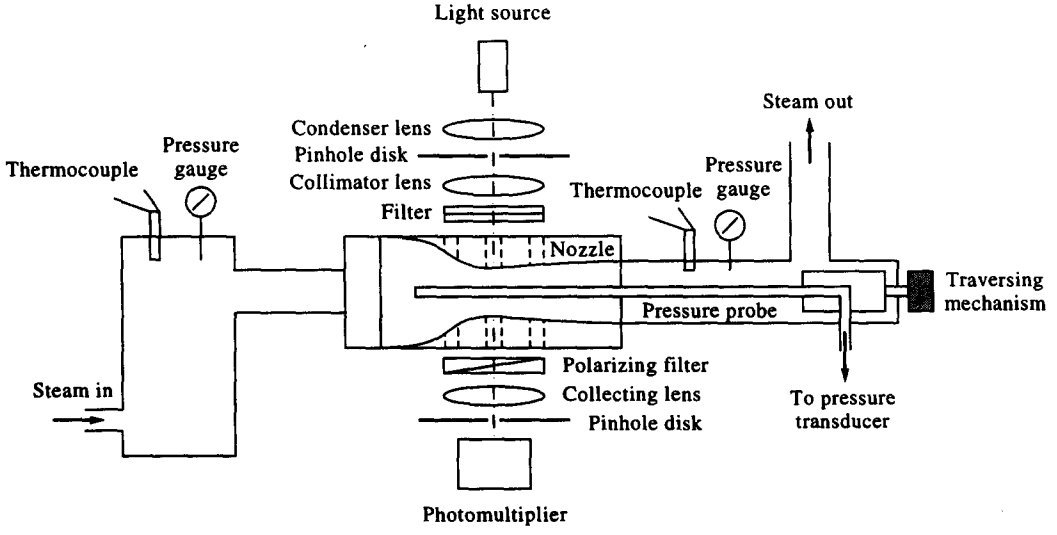


Figure 1.

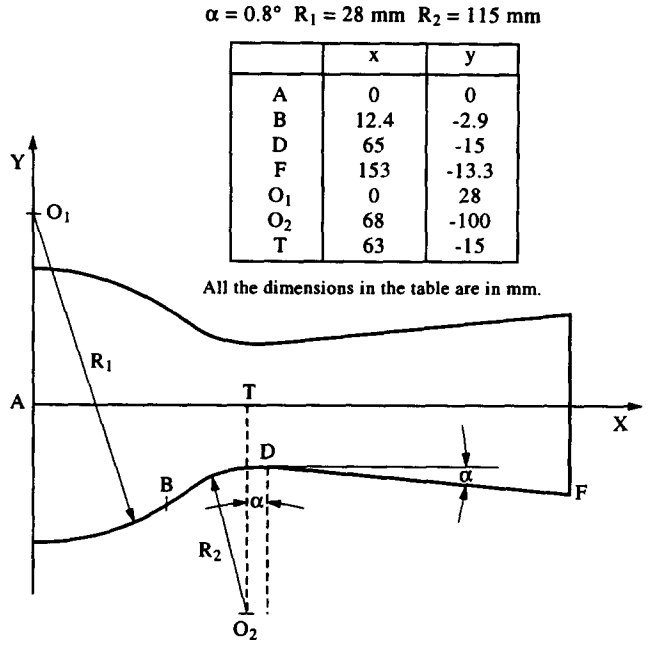


| | x | y |
|---|---|---|
| A | 0 | 0 |
| B | 12.4 | -2.9 |
| D | 65 | -15 |
| F | 153 | -13.3 |
| $O_1$ | 0 | 28 |
| $O_2$ | 68 | -100 |
| T | 63 | -15 |

Figure 2.

Table 1. Stagnation pressures and temperatures of the steam used in the experiment

| | Levels 1 | 2 | 3 | 4 | 5 (for dry test) |
|---|---|---|---|---|---|
| $P_0 \times 10^{-5}$ (Pa) | 25.1 | 28.6 | 32 | 35.5 | 32 |
| $T_0$ (K) | 521 | 530 | 535 | 544 | 574 |

An optical method is employed to measure the droplet size. The light from a mercury lamp source is condensed by a lens on to the first pinhole, which is placed at the focus of the collimator lens so that a parallel beam traverses the suspension in the flow channel. The attenuated beam emerging from the steam channel is collected by a lens and a second pinhole is placed before its intensity is measured by means of a photomultiplier. Two filters are set for selecting a single wavelength from the incoming rays and a polarizing filter is used to protect the photomultiplier from

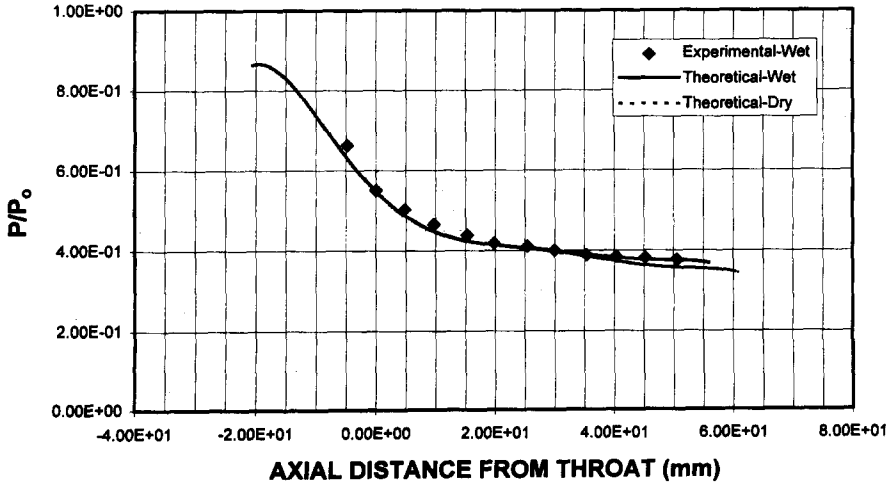


Figure 3. $P/P_0$ variation with nozzle length. $P_0 = 28.6$ Bar, $T_0 = 530$ K, $f = 0.02$, $\alpha = 0.8°$.

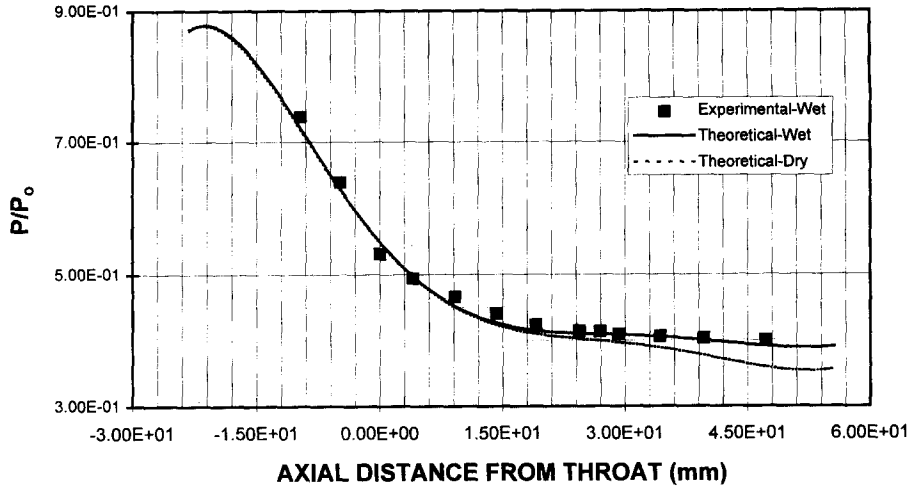


Figure 4. $P/P_0$ variation with nozzle length. $P_0 = 32$ Bar, $T_0 = 535$ K, $f = 0.02$, and $\alpha = 0.8°$.

overloading. It is known that light scattered by particles is concentrated more in the forward direction. It is indicated that collected scattered light will be negligible if the angle subtended by the diameter of each pinhole at its lens is less than $0.384/\alpha$ radians (Beyman 1990). $\alpha$ is the droplet size parameter defined as $\alpha = 2\pi r/\lambda$, where $\lambda$ is the wavelength of incident light and $r$ is the droplet radius. With lenses having a 100 mm focal length and the largest particle diameter assumed to be 1.8 $\mu$m and corresponding pinhole diameter is about 3 mm (Beyman 1990).

## 4. RESULTS AND DISCUSSION

The dry tests were carried out for two purposes: (i) to locate the position of the Wilson point which is often taken as the location where the dry and condensing static pressure plots first separate; and (ii) to adopt the correct value of the friction factor, which gives close results to the experimental measurements. The same value of the friction factor is then used for the analysis of wet tests.

The theoretical predictions together with the experimental results are shown in figures 3 and 4. In general, the agreement is considerably good. A departure of the dry curves from the wet curves is evident. This slow change is characteristic of the small rate of expansion in the nozzle. However, this process reverses at relatively low Mach numbers within short distance downstream of the

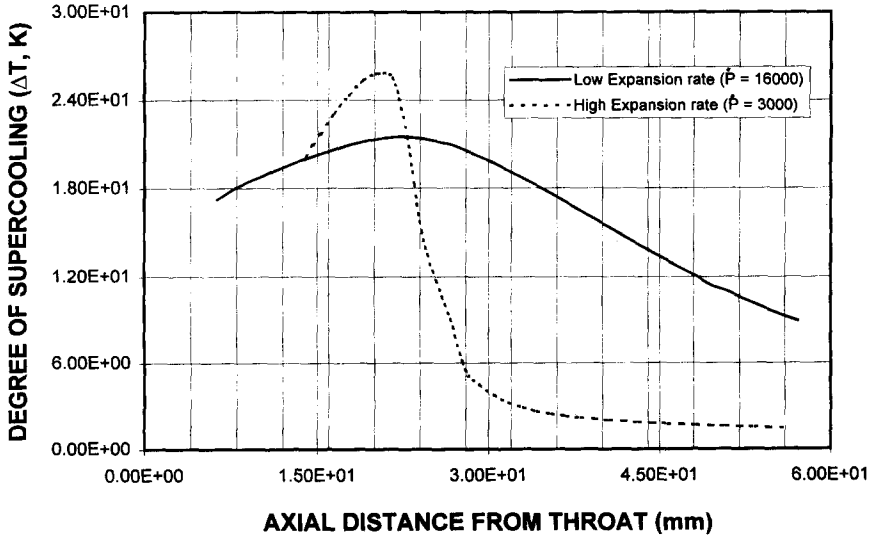


Figure 5. Variation in degree of supercooling along the nozzle.

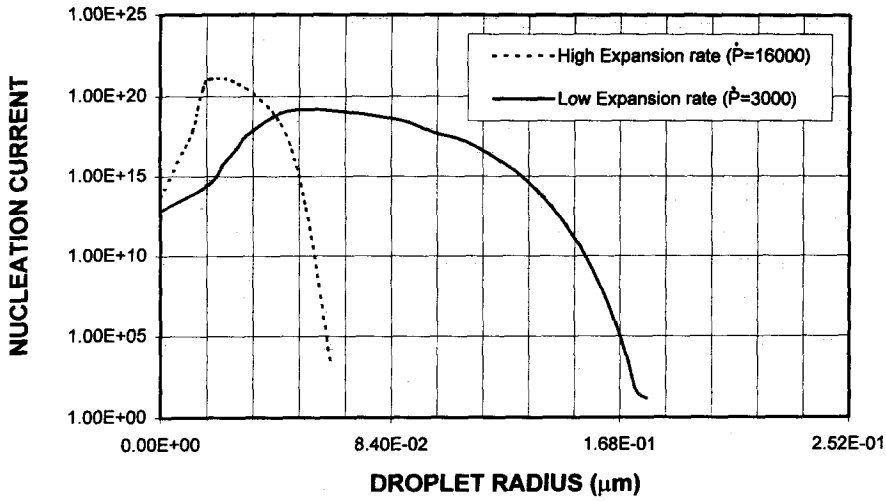


Figure 6. Variation in Nucleation current with droplet radius.

throat, in this case, the pressure rise associated with homogeneous condensation is easy to identify (figure 4). On the other hand, at small rates of expansion, steam supercools and reverts to equilibrium at a slower rate and the condensation zone is stretched over a longer distance. It can be seen from figure 5 that at low expansion rate ($\dot{P} = 1/P\ \mathrm{d}P/\mathrm{d}t$) the maximum degree of supercooling is 21.48 K at $x = 22.86$ mm and is relieved by 50% at about $x = 50.80$ mm, (i.e. over a distance of 27.94 mm). For high values of $\dot{P}$, the degree of supercooling is 25.36 K at $x = 19.05$ mm and is reduced to 11.73 K over a short distance of 6.35 mm. Therefore, at low expansion rate, the change in properties is spread over a large distance, which in turn results in difficulties in comparison of pressure distribution corresponding to low expansion and wet conditions.

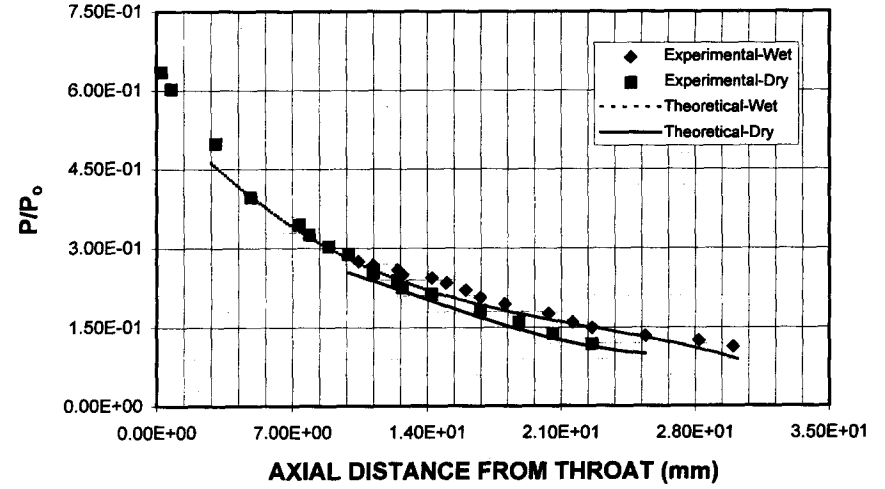


Figure 7. $P/P_0$ variation with nozzle length. $P_0 = 40.4$ Bar, $T_0 = 575$ K, $f = 0.02$, and $\alpha = 0.8°$.

Table 2. Values of Wilson parameters for experimental results

| $P_0$ (bar) | $T_0$ (K) | $P$ | $P^*$ (bar) | $P^*/P_s(T^*)$ | $T_s(P^*) - T$ | $r$ at 1% wetness ($\mu$m) | $x^*$ (mm) |
|---|---|---|---|---|---|---|---|
| 35.5 | 542 | 3419 | 14.7 | 1.614 | 21.5 | 0.165 | 22.86 |
| 32 | 535 | 3536 | 13.4 | 1.652 | 22 | 0.158 | 21.59 |
| 28.6 | 530 | 3004 | 11.35 | 1.702 | 22.4 | 0.194 | 30.48 |
| 21.1 | 521 | 3395 | 10.33 | 1.748 | 23.1 | 0.169 | 24.13 |

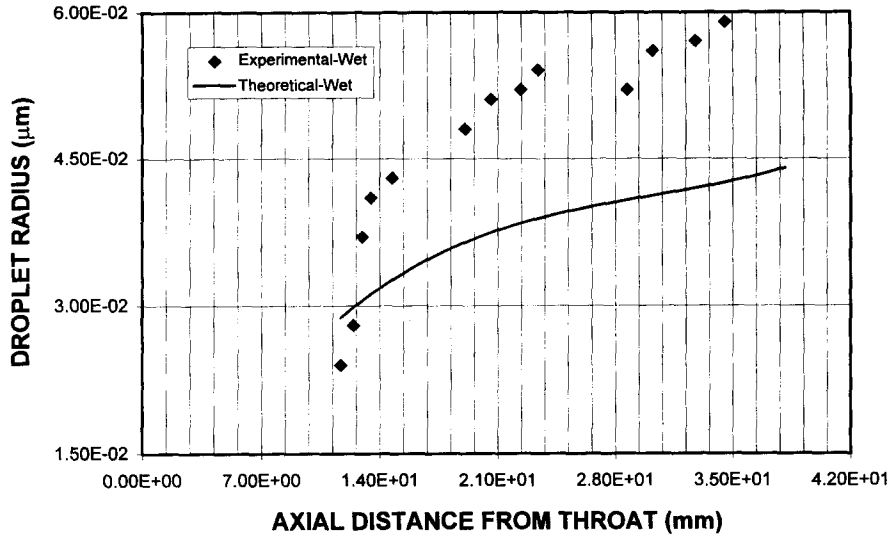


Figure 8. Droplet radius variation along the nozzle. $P_0 = 40.4$ Bar, $T_0 = 575$ K, $f = 0.02$, and $\alpha = 0.8^\circ$.

The main consequence of the small rate of change of pressure is to allow the very first centers of condensation generated to grow to a size large enough so that the latent heat released reduces the rate of increase of supercooling. The maximum of the nucleation current reaches value of the order of $10^{20}$; in this case, condensation occurs on small droplets (figure 5). It should be noted that the average droplet size corresponding to maximum nucleation current in the low expansion case is larger than that corresponding to high expansion rate and the same nucleation current, i.e. the theoretical droplet size corresponding to low expansion case is 0.052 $\mu$m, but this value reduces to 0.018 $\mu$m at high expansion rate.

Comparison of theoretical predictions and experimental results are shown in figures 6 and 7. The pressure distribution predicted and the location of condensation are in good agreement with the experimental results. The droplet radius predicted is approximately 25% less than the measured values. The discrepancies between the theoretical pressure distribution and the experimental results are small, but the initiation of condensation is predicted earlier than that corresponding to the measurement. This may be attributed to the uncertainties associated with the measurement errors.

The exact identification of the Wilson point presents some difficulty and no firm agreement exists about its location. However, the Wilson point is taken as the location where dry and condensing static pressure curves first separate and the nozzle isentropic efficiency is taken as 93%. The values

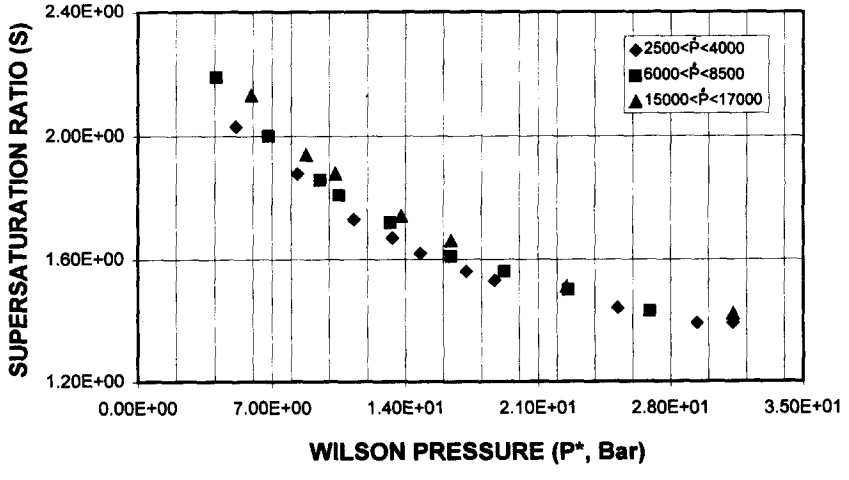


Figure 9. Variation of supersaturation ratio with Wilson point pressure.

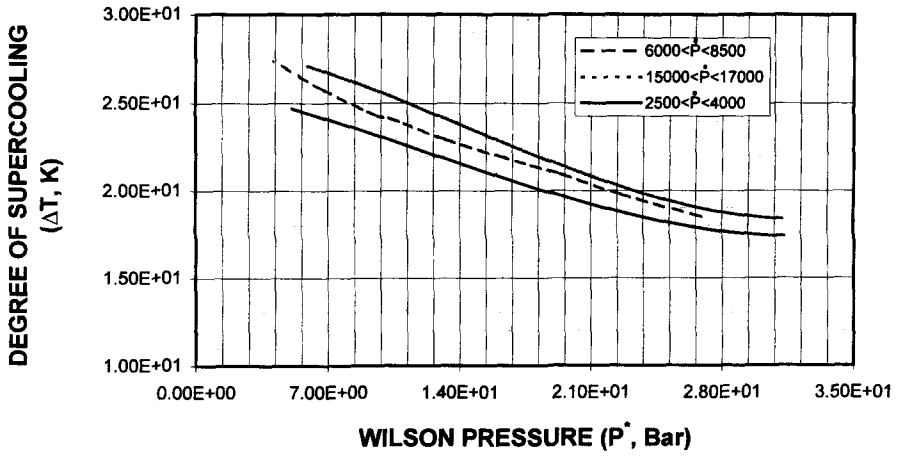


Figure 10. Variation in degree of supercooling with Wilson point pressure.

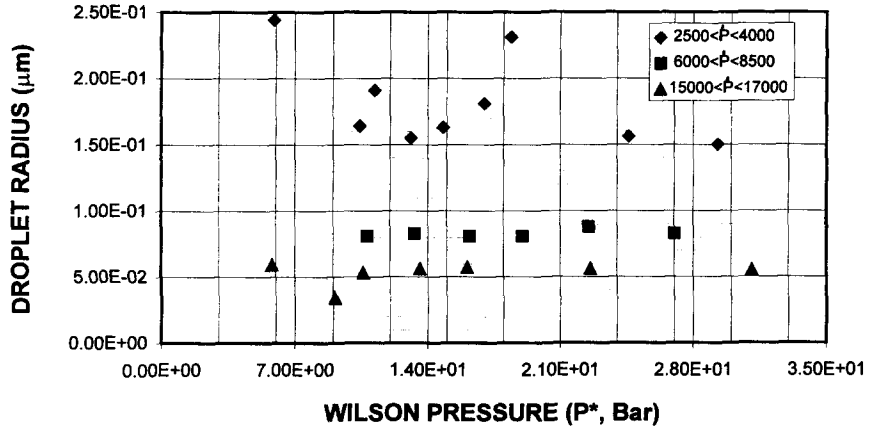


Figure 11. Variation of droplet radius with Wilson pressure.

of relevant parameters prevailing at the Wilson points are given in table 2. The value of the rate of expansion taken as 0.25 mm prior to the maximum supersaturation is almost constant.

The supersaturation ratio ($S^*$) and degree of supercooling ($\Delta T^*$) have been plotted with Wilson point pressure ($P^*$) in figures 8 and 9 (the supercript * indicates the critical conditions). $S^*$ and $\Delta T^*$ are influenced by the rate of expansion, but this effect is small. In this case, the initial centers of nucleation, which have sufficient time to grow at relatively small values of expansion rate, affect the subsequent history of the flow. The effect of pressure ($P^*$) is important in the case of low expansion rate. The average droplet radii computed are shown in figure 10 for a constant wetness of 1% and expansion rate and pressure as variables. The scatter of points for the low rate of expansion may be explained in terms of sensitivity of the droplet size with expansion rate. However, a consistent pattern can be seen indicating that droplet radius is inversely proportional to the rate of expansion. The trend of the curve in figure 10 has a low value of slope. This may be due to that during the initial stages of growth, the free molecular regime prevails which is extremely sensitive to pressure. After some time, the continuous regime becomes preponderant and the rate of growth of droplets slows down.

## 5. CONCLUSIONS

The kinetic theory approach for determining the rate of droplet growth has been developed successfully and the results predicted from theory and obtained from measurements are found to be in good agreement. The process of nucleation in high pressure steam can be described

satisfactorily by the model developed in the present study after introducing the suitable refinements to allow for the fluid effects.

There is a fall in the limiting amount of supersaturation as the pressure is increased, but the limiting condition also depends on the prevailing rate of expansion as well as any frictional reheat within the nozzle. The droplet diameter is found to be very sensitive to the expansion rate and the Wilson pressure.

It may be argued that if all the transport properties are calculated from the same model of the kinetic theory, the results will be mutually compatible and the problem will be resolved. To this end an examination is made of all available kinetic theories and it is found that because of the underlying physical difficulties, none of the theoretically based models is adequate to deal with the wetness problem. Therefore, a new expression is developed for the growth rate of droplets in both free and continuum flow regimes.

The presently introduced approach may be useful to explore the wetness problem relevant to the steam flow at different stagnation and static conditions.

## REFERENCES

Bahter F. and Heaton A. V. (1988) On the dissimilarities in wet steam behavior in model and full-scale turbines. In *Proceedings of BNES Conference on Technology of Turbine Plant Operating with Wet Steam*, London, October 1988.

Beyman J. (1990) *Waves and Optics*, 2nd Ed. Macmillan Educational Ltd, London.

Campbell W. W. (1964) Steam, the substance and its properties. In *Proc. Convention on Steam Plant Engineering*, I. Mech. E., pp. 1–6.

Collier J. (1981) *Convective Boiling and Condensation*, 2nd Ed. McGraw-Hill, New York.

Courtney W. G. (1962) Remarks on homogeneous nucleation. *J. Chem. Phys.* **36,** 2009–2013.

E. S. D. (Engineering Science Data) (1978) Thermal cond. of ice, water and steam, Item 78039.

Filipov G. A., Povorov O. A., Dikarev V. I., Nikolskii A. I. and Semenyuk A. V. (1980) Investigation of power and flow characteristics of annular turbine cascades operating on wet steam. *Thermal Engineering* **27,** 626–630.

Frenkel J. (1946) *Kinetic Theory of Liquids*. Oxford University Press, London.

Kantrowitz A. (1951) Nucleation of very rapid vapor expansion. *J. Chem. Phys.* **19,** 1097–1102.

Labuntsov D. A., Lobaehe A. G., Kolchugin B. A. and Zakharova E. A. (1984) The main principles of variation in vapor content of equilibrium and non-equilibrium two-phase flows in channels of different geometry. *Thermal Engineering* **31,** 506–508.

Lokshin V. A., Kreidin I. L. and Kreidin B. L. (1984) Experimental investigation of hydraulic resistance with condensation of steam down-flow inside a vertical tube. *Thermal Engineering* **31,** 21–24.

Tatsuno K. and Nagao S. (1986) Water droplet size measurements in an experimental steam turbine using an optical fiber droplet sizer. *J. Heat Transfer* **108,** 939–945.

Yeoh C. C. and Young J. B. (1984) Non-equilibrium throughflow analysis of low pressure wet steam turbines. *Trans. ASME, J. Engrg Power* **106,** 716–721.

Young J. B. (1991) The condensation and evaporation of liquid droplets in a pure vapour at arbitrary Knudsen number, *Int. J. Heat Mass Transfer* **34,** 1649–1661.

## APPENDIX

The equations governing the thermodynamic properties of superheated vapor need to be extrapolated. The thermodynamic properties of the steam can be deduced from the equation of state, the saturation line and the specific heat at zero pressure. It should be noted here that rapid change in the properties near the saturation line is caused by the change in the concentration of the molecular clusters. It has been shown that the corrected cluster concentration on the pressure of a system are negligible and that the Vukalovitch equation (Campbell 1964) is still valid with negligible error (Collier 1981).

*Equation of state*

The equation of state developed by Vukalovitch (Campbell 1964) for the pressure range 0.00981–98.1 bars is

$$\frac{P}{\rho_G R T_G} = 1 - B_1\rho_G + B_2\rho_G^2 + B_3\rho_G^3. \qquad [A1]$$

The coefficients $B$ are defined by

$$B_1 = -\frac{e}{RT_G} - \phi_1 + b,$$

$$B_2 = -b\phi_1 + 4\phi_1^2\phi 2,$$

$$B_3 = 32b\phi_1^2\phi_2,$$

where

$$\phi_1 = \frac{CR}{T_G^{w_1}} \quad \text{and} \quad \phi_2 = 1 - \frac{K}{T_G^{w_2}}$$

and

$$e = 63.2\ \text{m}^5/(\text{kg s}^2), \quad b = 0.00085\ \text{m}^3/\text{kg}, \quad C = 0.3977 \times 10^6,$$

$$R = 461.4\ \text{J/(kg K)}, \quad K = 22.7, \quad w_1 = \frac{3 + 2m_1}{2},$$

$$w_2 = \frac{3m_2 - 4m_1}{2}, \quad m_1 = 1.968, \quad m_2 = 2.957.$$

Defining

$$\chi = \frac{\rho_G}{P}\left(\frac{\partial P}{\partial \rho_G}\right)_{T_G}$$

and

$$X = \frac{T_G}{P}\left(\frac{\partial P}{\partial T_G}\right)_{\rho_G}$$

and recalling that the differential form of the equation of state can be written as

$$\frac{dP}{P} - \chi\frac{d\rho_G}{\rho_G} - X\frac{dT_G}{T_G} = 0, \qquad [A2]$$

where

$$\chi = 1 + \frac{B_1\rho_G + 2B_2\rho_G^2 + 3B_3\rho_G^3}{1 + B_1\rho_G + B_2\rho_G^2 + B_3\rho_G^3},$$

$$X = 1 - \frac{T_G}{1 + B_1\rho_G + B_2\rho_G^2 + B_3\rho_G^3}\left(\rho_G\frac{dB_1}{dT_G} + \rho_G^2\frac{dB_2}{dT_G} + \rho_G^3\frac{dB_3}{dT_G}\right).$$

Equation [A2] together with the definitions of $\chi$ and $X$ is valid for equations of state truncated at any virial coefficient.

*Specific heat at constant pressure*

The specific heat at constant pressure may be obtained from

$$\left(\frac{\partial h}{\partial P}\right)_{T_G} = v - T_G\left(\frac{\partial v}{\partial T_G}\right)_P.$$

Therefore

$$c_P = \frac{\partial}{\partial T}\int\left[v - T_G\left(\frac{\partial v}{\partial T_G}\right)_P\right]dP + f_c(T).$$

After substitution of $v$ from the equation of state, the integration can be easily carried out. The constant of integration $f_c(T)$ is determined by setting $P = 0$ and using the value of $c_{P_0}$ (Tatsuno and Nagao 1986). Therefore, the equation for $c_P$ yields

$$c_P = -RT_G\left[\frac{1}{T_G}\left(\frac{1}{v}\frac{dB_1}{dT_G} + \frac{1}{2v^2}\frac{dB_2}{dT_G} + \frac{1}{3v^3}\frac{dB_3}{dT_G}\right) + \left(\frac{1}{v}\frac{d^2B_1}{dT_G^2} + \frac{1}{2v^2}\frac{d^2B_2}{dT_G^2} + \frac{1}{3v^3}\frac{d^2B_3}{dT_G^2}\right)\right]$$

$$+1.111 + 0.00071T_G + \frac{6992}{T_G^2}\left(\frac{kJ}{kgK}\right).$$

The specific heat capacity at constant volume ($c_v$) can be written as

$$c_P - c_v = T\left(\frac{\partial P}{\partial T}\right)_v\left(\frac{\partial v}{\partial T}\right)_P$$

or rearrangement gives

$$c_v = -2RT_G\left[\frac{1}{T_G}\left(\frac{1}{v}\frac{dB_1}{dT_G} + \frac{1}{2v^2}\frac{dB_2}{dT_G} + \frac{1}{3v^3}\frac{dB_3}{dT_G}\right) - \frac{1}{2}\left(\frac{1}{v}\frac{d^2B_1}{dT_G^2} + \frac{1}{2v^2}\frac{d^2B_2}{dT_G^2} + \frac{1}{3v^3}\frac{d^2B_3}{dT_G^2}\right)\right]$$

$$+1.111 + 0.00071T_G + \frac{6992}{T_G^2}\left(\frac{kJ}{kgK}\right).$$

*Specific heat ratio (k)*

$k$ is defined as

$$k = -\frac{v}{P}\left(\frac{\partial P}{\partial v}\right)_S.$$

Using Maxwell's relations and rearranging result

$$k = -\frac{v}{P}\left(\frac{\partial P}{\partial v}\right)_T\frac{c_P}{c_v}.$$

Using the equation of state for $(\partial P/\partial v)_T$ yields

$$k = \frac{v}{P}\left[RT_G\left(\frac{1}{v^2} + \frac{2B_1}{v^3} + \frac{3B_2}{v^4} + \frac{4B_3}{v^5}\right)\right]\frac{c_P}{c_v}.$$

Table A1. Variation of diffusion coefficients with flow properties

| $P$ (kPa) | $\ln P$ | $T_L$ (K) | $D/\sqrt{T_L}$ | $-\ln(D/\sqrt{T_L})$ |
|---|---|---|---|---|
| 6.895 | 1.9308 | 311.9 | $5.28661 \times 10^{-6}$ | 12.15033 |
| 27.579 | 3.31705 | 340.4 | $1.53918 \times 10^{-6}$ | 13.38426 |
| 68.948 | 4.23335 | 362.7 | $7.49448 \times 10^{-7}$ | 14.10393 |
| 275.79 | 5.61964 | 403.8 | $2.36243 \times 10^{-7}$ | 15.2584 |
| 689.48 | 6.53594 | 437.5 | $1.07541 \times 10^{-7}$ | 16.04539 |
| 2757.9 | 7.92222 | 502.4 | $2.8995 \times 10^{-8}$ | 17.35614 |

*Specific enthalpy*

From the first and second law of thermodynamics

$$\left(\frac{\partial h}{\partial P}\right)_T = v - T_G\left(\frac{\partial v}{\partial T_G}\right)_P$$

which can be integrated to give

$$h = \int\left[v - T_G\left(\frac{\partial v}{\partial T_G}\right)_P\right]dP + f_{h(T_G)}$$

and

$$f_{h(T_G)} = \int f_c(T_G)dT + \text{constant.}$$

The constant of integration is arbitrary, but usually it is set to zero at 0°C for the saturated liquid. The expected value of $h$ at 100°C, saturated vapor, is 2676 kJ/kg. Substitution of equation of state into above equation yields

$$h = -RT_G\left[\frac{1}{v}\frac{dB_1}{dT_G} + \frac{1}{2v^2}\frac{d1B_2}{dT_G} + \frac{1}{3v^3}\frac{dB_3}{dT_G}\right]$$
$$+1.1111T_G + 3.5588 \times 10^{-4}T_G^2 - \frac{6992}{T_G} + Pv + 2070.54\left(\frac{kJ}{kg}\right).$$

*Relation between the diffusion coefficients*

From kinetic theory, it is evident that $D$ is proportional to the mean molecular velocity ($\bar{c}$), which is proportional to the square root of temperature. Therefore

$$\frac{D_G}{D'} \propto \sqrt{\frac{T_G}{T'}}. \qquad [A3]$$

It was shown previously that

$$\frac{dM}{dt} = 4\pi R^2(\rho_G D_G - \rho D'), \qquad [A4]$$

where $M$ is the mass of the droplet of radius $r$. Substitution of $D_G$ from [A4] into [A3] gives

$$D' = \frac{dM/dt}{4\pi r(\rho_G\sqrt{T_G/T'} - \rho')}. \qquad [A5]$$

This is the value of the diffusion coefficient at the droplet surface. To calculate this coefficient at any other location, [A4] can be integrated between $R = r$ and $R = R$, which after rearrangement becomes

$$D_R = \frac{\rho'}{\rho R}D' + \frac{dM/dt}{4\pi}\left(\frac{1}{r} - \frac{1}{R}\right).$$

It should be noted that in [A5] pressure equilibrium is assumed.

The effect of pressure may be included by repeating the above procedure for a large number of conditions. In this case, the pressure was varied from 0.07 to 27 bar and the vapor temperature from 45°C supercooling to 45°C superheat. A plot of resulting values of $\log(D/\sqrt{T})$ against log $P$ indicates that the following relation can be written

$$\log\left(\frac{D}{\sqrt{T}}\right) = \log C - n \log P$$

A set of specimen calculations is given in table A1. Values of mass flux calculated using this expression are found to be in agreement with those obtained from heat transfer analysis to within 15%. When calculating the growth of droplets immersed in supercooled water, it is essential that the expression developed above should be used in conjunction with the equation of state and expression for the thermal conductivity adopted in this investigation.